Research article

Journal of RAMAN SPECTROSCOPY

Received: 11 September 2012 Revised: 9 November 2012 Accepted: 31 December 2012 Published online in Wiley Online Library: 31 March 2013

(wileyonlinelibrary.com) DOI 10.1002/jrs.4255

Connection between the vibrational dynamics and the cross-linking properties in cyclodextrins-based polymers†

Vincenza Crupi,[a] Aldo Fontana,[b,c] Marco Giarola,[d] Domenico Majolino,[a] Gino Mariotto,[d] Andrea Mele,[e] Lucio Melone,[e] Carlo Punta,[e] Barbara Rossi,[b,d]* Francesco Trotta[f] and Valentina Venuti[a]

The vibrational dynamics of a new class of cross-linked polymers obtained from both native and modified cyclodextrin, referred to as cyclodextrin nanosponges, is here investigated. The main purpose is to spot the structure of these materials at molecular level unlikely to be characterized by diffraction methods due to the low or null degree of crystallinity. The analysis of the spectral features of the vibrational bands observed between 1650 and 1800 cm^{-1} in both Raman and infrared spectra, and assigned to the carbonyl stretching modes of the polymeric network, is performed by using band deconvolution procedures. At the same time, a detailed inspection of the low-wavenumber vibrational dynamics of these polymers is carried out, focusing on the modifications occurring on the so-called boson peak.

The simultaneous analysis of different wavenumber ranges in Raman and infrared spectra of cyclodextrin nanosponges allows us to develop a reliable strategy for exploring both the cross-linking degree and the elastic properties of these innovative materials. The overall results give a complete characterization of the structural and dynamical properties of the system, in turn strictly connected to the entrapment/transport ability of these polymeric matrices. Copyright © 2013 John Wiley & Sons, Ltd.

Keywords: cyclodextrin; polymers; boson peak; cross-linking; C=O stretching

Introduction

Among the many systems that have been proposed in recent years as efficient carriers for the transport of bioactive molecules, some classes of polymers have found important applications in the field of drug delivery due to their properties of biocompatibility, biodegradability, and the possibility to be easily functionalized.

In particular, polymeric networks made up of cross-linked synthetic and/or natural macromolecules[1] have attracted great interest as precursors for designing new soft materials with properties tailored for specific applications in many field, ranging from drug delivery[2] to tissue engineering and regenerative medicine.[3,4]

In this scenario, the deep knowledge of the cross-linking properties of the final polymeric structure is a mandatory step to control and design the entrapment/transport ability inside the matrix. Nevertheless, carrying out a systematic structural and dynamical characterization of cross-linked polymeric networks suffers from many intrinsic difficulties. This fact is mainly due to the random nature of the growing process of the polymer and their amorphous nature that seriously hampers the use of diffraction techniques as main structural investigation methods.

Cyclodextrins (CD) are natural cyclic oligosaccharides with a characteristic structure of a truncated cone, with an internal hydrophobic cavity and an outer hydrophilic surface. They are well known for their ability to form noncovalent inclusion complexes with a variety of organic molecules, thus altering the chemical and physical properties of the guest molecule.[5–8] This characteristics makes CD particularly suitable for applications as carrier systems of active molecules, thanks to their ability to increase the rate of solubilization, the solubility, and stability of the active ingredient.

More recently, many efforts have been devoted to develop and produce new organic systems, based on CD, with the aim to improve the performance of natural CD as host systems.[9] In particular, a new class of materials has been recently patented

* Correspondence to: Barbara Rossi, Dipartimento di Fisica, Università di Trento, via Sommarive 14, 38123 Povo, Trento and IPCF CNR, UOS Roma, I-00185 Roma, Italy. E-mail: rossi@science.unitn.it

† This article is from the GISR part of the joint special issue on the European Conference on Nonlinear Optical Spectroscopy (ECONOS 2012) with Guest Editors Johannes Kiefer and Peter Radi and the II Italian Conference of the National Group of Raman Spectroscopy and Non-Linear Effects (GISR 2012) with Guest Editor Maria Grazia Giorgini.

a Dipartimento di Fisica, Università di Messina, and CNISM, UdR Messina, Viale Ferdinando Stagno D'Alcontres 31, 98166 Messina, Italy

b Dipartimento di Fisica, Università di Trento, via Sommarive 14, 38123 Povo, Trento, Italy

c IPCF CNR, UOS Roma-00185, Italy

d Dipartimento di Informatica, Università di Verona, Strada le Grazie 15, 37134 Verona, Italy

e Department of Chemistry, Materials and Chemical Engineering "G. Natta", Politecnico di Milano, Piazza L. Da Vinci, 32 20133 Milano, Italy

f Dipartimento di Chimica, Università di Torino, Via P. Giuria 9, 10125 Torino, Italy

in which the monomer units constituted by CD, linked via carbonate groups, form highly cross-linked polymers, referred to as CD nanosponges (CDNS).[10–13] The nanoporous structure of CDNS shows a network of both CD lyphophilic cavities and more hydrophilic channels, and it is characterized by the ability to encapsulate a large variety of substances, modifying its physicochemical properties. These features make CDNS highly attractive for several applications in different fields, such as in environmental control as absorbant for polluting wastes[14,15] and in pharmaceutical field, as nanovehicles capable of active transport increasing bioavailability and solubility of drugs.[16–20]

Despite that CDNS have been shown to be a promising carrier system for many types of active molecules, the thorough physicochemical and structural characterization of these polymers is still incomplete. The molecular structure of nanosponges obtained by reacting CD with a suitable polyfunctional agent such as pyromellitic dianhydride (PMA)[21–23] and carbonyldiimidazole (CDI)[22,24,25] was investigated by using inelastic light-scattering techniques, infrared (IR) spectroscopy, quantum chemical simulations, and nuclear magnetic resonance techniques. These studies seem to suggest that the type and the molar ratio of cross-linking agent with respect to the monomers used during the synthesis of CDNS can significantly modulate the cross-linking properties of the polymers, in turn related to important parameters such as the swelling capacity and the hydrophilicity/hydrophobicity of the final product.

The present paper reports on the investigation of the vibrational dynamics of a new type of CDNS, obtained by polymerization of CD with the cross-linking agent ethylenediaminetetraacetic acid (EDTA) at different CD/EDTA molar ratios. The combined use of IR and Raman spectroscopies in different wavenumber ranges (1–100 and 1600–1800 cm^{-1}) allows us to inspect the spectral properties of the bands arising from intramolecular vibrational modes, i.e. C=O stretching vibrations, and of the so-called boson peak (BP), a prominent feature typically found in the low-wavenumber Raman spectra of disordered systems.[26–35] By following this approach, we are able to simultaneously explore the connectivity degree of the polymer network and the elastic properties (i.e. stiffness) of the material, over a mesoscopic length scale, giving a complete structural characterization of the system.

Experimental methods

Synthesis of CDEDTA nanosponges

The nanosponges were obtained following a synthetic procedure previously reported.[10,11,16] To obtain β-CDEDTA1*n* nanosponges, anhydrous β-CD (1.135 g – 1 mmol) was dissolved at room temperature in anhydrous dimethyl sulfoxide (4 ml) containing 1 ml of anhydrous Et_3N. Then, the cross-linking agent EDTA dianhydride (EDTAn) was added at molecular ratios of 1:*n* (with $n = 4,6,8,10$) under intense stirring. The polymerization was complete in few minutes obtaining a solid that was broken up with a spatula and washed with acetone in a Soxhlet apparatus for 24 h. The pale yellow solid was finally dried under vacuum.

The synthesis of Hp β-CDEDTA14 was performed in similar way, using 1.380 g (1 mmol) of anhydrous (2-hydroxypropyl)-βCD (Fluka, average M_w: 1,380 Da – 0.6 molar substitution) and 4 mmol of EDTAn.

Raman scattering measurements

All the Raman spectra were recorded on dried samples deposited on a glass slide, in air, and at room temperature. All the spectra were carried out in backscattering geometry, in crossed polarization, by using two different experimental setups to better explore different spectral ranges.

For the spectra collected in the wavenumber range between 100 and 3700 cm^{-1}, the exciting radiation at 632.8 nm (He–Ne laser, power at the output ≈20 mW) was focused onto the sample surface with a spot size of about 0.8 μm^2 through the 100× objective (NA = 0.9) of a microprobe setup (Horiba-Jobin-Yvon, LabRam Aramis) consisting of a 46-cm focal length spectrograph using a 1800 grooves/mm grating and a charge-coupled device detector. The elastically scattered radiation was filtered by using a narrow-band edge filter. The resolution was about 0.35 cm^{-1}/pixel.

Low-wavenumber Raman spectra of nanosponges were recorded over the wavenumber range between 1.3 and 400 cm^{-1} by using a triple-monochromator spectrometer (Horiba-Jobin Yvon, model T64000) set in double-subtractive/single configuration and equipped with holographic grating 1800 grooves/mm. Micro-Raman spectra were excited by the 647.1 nm wavelength of an argon/krypton ion laser and detected by a charge-coupled device detector cryogenically cooled by liquid nitrogen. Exciting radiation was focused onto the sample surface with a spot size of about 1 μm^2 through an 80× objective with NA = 0.75. The resolution was about 0.36 cm^{-1}/pixel.

The relative amplitude of the luminescence background observed in the Raman spectra is less than a few percent in all the samples examined. The experimental profiles were corrected for the luminescence background by subtracting an interpolating baseline modeled as a linear function.

Two Lorentzian functions centered at about 1730 and 1750 cm^{-1} were used to fit the Raman spectra in the C=O stretching region. A fitted range of about 200 cm^{-1} (1650–1850 cm^{-1}) was considered. For each fitting session, multiple iterations were performed until a converging solution is reached and the value of chi-square is minimized.

FTIR–ATR measurements

Fourier transform IR spectroscopy (FTIR)–attenuated total reflectance (ATR) absorption measurements were performed on dried samples, in the 600–4000 cm^{-1} wavenumber range and at room temperature. Spectra were recorded using a Bomem DA8 Fourier transform spectrometer, operating with a Globar source, in combination with a KBr beamsplitter, a DTGS/KBr detector. The powders were contained in Golden Gate diamond ATR system, just based on the ATR technique. The spectra were recorded in dry atmosphere, to avoid dirty contributions, with a resolution of 2 cm^{-1}, automatically adding 100 repetitive scans to obtain a good signal-to-noise ratio and a high reproducibility. All the IR spectra were normalized for taking into account the effective number of absorbers. No mathematical correction (e.g. smoothing) was done, and spectroscopic manipulation such as baseline adjustment and normalization were performed using the SpectraCalc software package GRAMS (Galactic Industries, Salem, NH, USA). For the C=O spectral profile, second derivative computations, not reported here, have been used for evaluating the wavenumbers of the maxima of the different sub-bands.

Journal of RAMAN SPECTROSCOPY

The presence, in the experimental spectra, of two sub-bands for the C=O stretching region with the assigned center frequencies was suggested by the two minima observed in the second derivative profiles approximately corresponding to the maxima of each band component. Band decomposition was then undertaken, by multiple curve fitting into Voigt profiles applied to the experimental spectra based on these wavenumber values. We used the routine available in the PeakFit 4.0 software package. The statistical parameters defined in the software manual were used as a guide to 'best-fit' iteration until a converging solution is reached. Although the spectral decomposition procedures have no unique solution, we remark that the one we adopted here uses the minimum number of free parameters and, at the same time, it furnishes extremely good fits to the data. The best fit is, in fact, characterized by $r^2 \approx 0.9999$ for all the investigated systems.

Results and discussion

In Fig. 1(a) and (b), the typical Raman and FTIR–ATR spectra of β-CDEDTA14 observed in the wavenumber range 1680–1800 cm^{-1} are reported. A characteristic asymmetric band centered at about 1740 cm^{-1} in both Raman and IR spectra is found in this spectral range for all the samples of EDTA-nanosponges examined. This band arises from intermolecular vibrational modes of the polymeric network, and on the basis of the comparison with the vibrational spectra of PMA-nanosponges,[23] it can be reasonably assigned to the carbonyl stretching vibrations of esterified EDTA. In fact, in the spectral range 1600–1800 cm^{-1}, CD molecules do not show any interfering bands; thus, the spectral region reported in Fig. 1 contains the vibrational modes of carbonyl EDTA only.

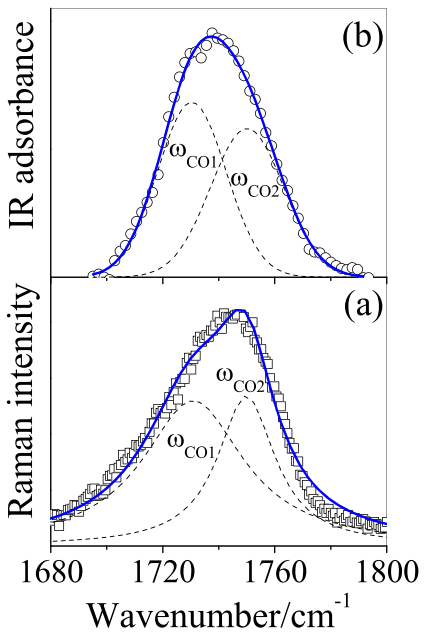

Figure 1. Experimental Raman (a) and FTIR-ATR (b) spectra for β-CDEDTA14 in the 1680–1800 cm^{-1} wavenumber range, together with the best-fit (continuous line) and the deconvolution components (dashed lines).

A well-assessed curve fitting procedure[23,25,36] was employed, in order to allow the deconvolution of the band observed between 1680 and 1800 cm^{-1} into its individual spectral components. The observation of two minima in the second derivative profiles of the experimental spectra suggests the presence of at least two sub-bands for the C=O stretching region. Band decomposition was then undertaken, by multiple curve fitting applied to the Raman and IR spectra. Two different mathematic functions (Voigt distribution functions for IR and Lorentzian peaks for Raman profile, respectively) were used for the fitting of the experimental data.

By following this approach, two spectral components for the C=O stretching band were identified, i.e. ω_{CO1} falling at $\approx$1730 cm^{-1} and ω_{CO2} found at $\approx$1750 cm^{-1} in both Raman and IR spectra. These sub-bands describe the existing types of two carbonyl stretching modes assigned, respectively, to the vibrations of the C=O belonging to the ester groups (ω_{CO1}) and to the free carboxylic groups (ω_{CO2}) of EDTA. This assignment is supported by the results of quantum chemical computations performed on the more simply model of esterified PMA, which mimics the molecular environment of PMA after the reaction with the OH groups of CD to form the polymeric network of PMA-nanosponges.[23] Moreover, the observed discrepancy of about 20 cm^{-1} between the wavenumber position of the two sub-bands of the C=O profile in EDTA-nanosponges (ω_{CO1} = 1730 cm^{-1} and ω_{CO2} = 1750 cm^{-1}) is consistent with the entity of the energy shift found between the modes assigned, respectively, to the stretching vibrations of the C=O belonging to the ester groups (1705 cm^{-1}) and to the carboxylic groups (1726 cm^{-1}) of the bridging molecule in the case of PMA-nanosponges.[23]

It is noteworthy that, in principle, both the carbonyl groups ω_{CO1} and ω_{CO2} could be equally involved in hydrogen bonds networks with the free OH groups of CD molecules. This occurrence could lead to a general shift to lower wavenumber of each spectral component, i.e. of the total C=O stretching profile, which is in turn ascribed to a weakening of the double bond in the corresponding carbonyl groups because of the establishment of stronger forces. On the other side, the separation of these additional spectral components can become not meaningful because of strong overlapping of the bands.

On the basis of these considerations, we are confident that each of the two sub-bands ω_{CO1} and ω_{CO2} can reasonably account for both the contributions arising from hydrogen-bonded and nonhydrogen-bonded types of carbonyl group (ester and carboxylic).

The total estimated intensity for the C=O stretching band is directly proportional to the population of the C=O functional groups, in turn related to the cross-linking degree of the polymeric network of EDTA-nanosponges. This estimated intensity can be conveniently used as a semi-quantitative descriptor of the cross-linking degree of the system, after a preliminary normalization of the vibrational spectra to the intensity of the bands at ~1015 and 2903 cm^{-1} for IR and Raman data, respectively.[23,25]

These vibrational modes are, respectively, assigned to the stretching vibrations of C–O and CH_2 groups of the CD units. These chemical groups are not involved in polymerization with EDTA, and moreover, the intensity of their corresponding vibrational bands does not suffer from complexation phenomena between free EDTAn and CD, which are to be excluded due because of the polarity of the cross-linker molecules.

On the basis of these arguments, we are confident that the bands at ~1015 and 2903 cm^{-1} in IR and Raman spectra can be conveniently used as reliable internal references for evaluating the relative number of cross-linkers with respect to CD molecules present in the polymeric network of nanosponges.

In Fig. 2(a) and (b), the total intensity $I_{CO1} + I_{CO2}$ of the C=O stretching band observed in Raman and IR spectra, respectively, is shown as a function of the CD:EDTA molar ratio *n*. The values of total intensity are estimated as the sum of the intensities of the two different spectral components I_{CO1} and I_{CO2}, in which the C=O vibrational band has been deconvoluted by using fitting procedure.

A maximum corresponding to a sixfold excess of cross-linking agent EDTA with respect to β-CD is observed in both the plots of Fig. 2(a) and (b), whereas for molar ratios $n > 6$, the reticulation in the polymeric network tends to decrease, probably because of the occurrence of steric effects that prevent further cross-linking of the polymer.

In Fig. 2(c) and (d), the ratio between the intensity of the two spectral components of the C=O stretching band is plotted as a function of *n*. Because the type of vibration for the two types of carbonyls evidenced in the EDTA moiety is practically the same, namely C=O stretching mode,[23] we can reasonably assume that the experimental intensities I_{CO1} and I_{CO2} are directly proportional to the population of corresponding types of oscillators, ω_{CO1} and ω_{CO2}. Thus, the intensity ratio I_{CO1}/I_{CO2} reflects the relative amount of ester and carboxylic groups in polymeric network, estimated by Raman and IR spectra (Fig. 2 (c) and (d), respectively). The excess of ester bonds with respect to the free carboxylic groups appears to be maximum for $n = 6$. This fact suggests that the sixfold excess of EDTA with respect to β-CD tends to give a saturation effect for the three-dimensional growth of the polymer, as already found for PMA-nanosponges.[22,23]

By inspection of Fig. 2, we can also infer that the degree of reticulation for EDTA nanosponges for $n < 6$ seems to be slightly dependent on the chemical modifications of CD macrocycle, as observed by comparing the intensity of the C=O stretching band estimated for β-CDEDTA and Hpβ-CDEDTA at molar ratio $n = 4$.

Finally, it is also to be noted that a relative good agreement is found between Raman and IR results, thus confirming the reliability of the data treatment and normalization procedure employed.

Complementary information on the elastic properties of polymeric network of nanosponges can be obtained by the analysis of low-wavenumber vibrational dynamics of the material.[22] In Fig. 3, the Raman spectrum of β-CDEDTA18 is reported in the wavenumber range between 0 and 200 cm^{-1}, as an example.

Three main contributions can be observed in the spectra of EDTA nanosponges in this spectral region: a quasi-elastic (QE) scattering component, a broad asymmetric bump peaked at about 25–35 cm^{-1}, which is referred to as the BP, and a higher-wavenumber inelastic vibrational component found at about 80 cm^{-1}. As already mentioned,[22] the BP is a characteristic bump typically found in low-wavenumber inelastic neutron and Raman scattering spectra of a large variety of amorphous materials,[26–35] which is associated to an excess in the vibrational density of states over the Debye level. The BP has been claimed to be a universal feature of disordered systems and it appears to be connected to significant physical parameters, including the elastic properties of the system on a mesoscopic length scale.[22,27,29,31–35] In fact, recent studies performed also on polymeric systems[22,31–34] suggested the existence of a clear-relationship between the elastic properties of material and the position of the maximum of BP, which tends to move to higher energies when the stiffness of the system increases.[28,30,35]

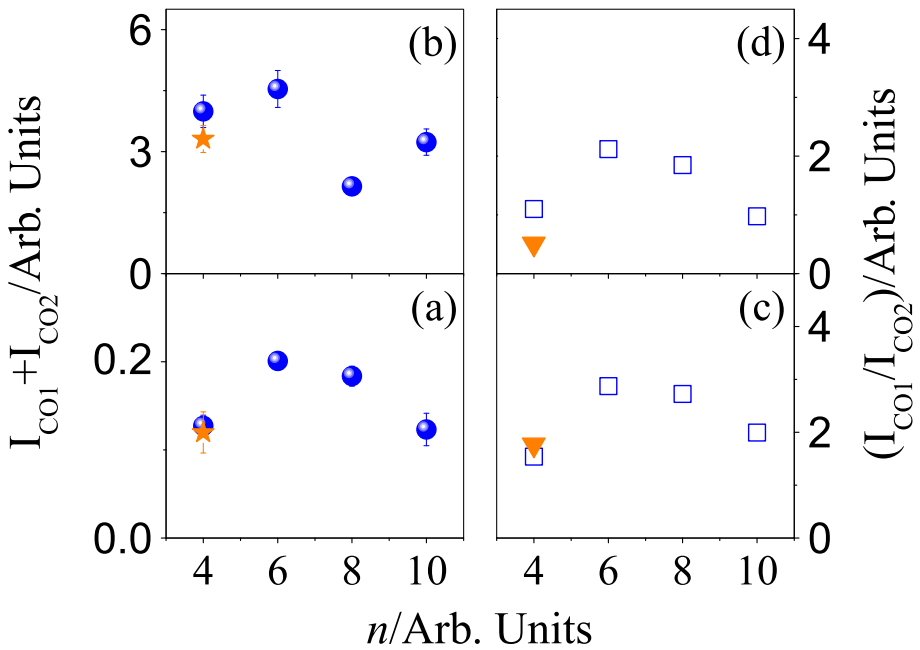

Figure 2. Total intensity $I_{CO1} + I_{CO2}$ and ratio I_{CO1}/I_{CO2} between the intensity of the two spectral contributions to the C=O stretching band observed in Raman (a) and (c) and FTIR-ATR (b) and (d) spectra, as a function of *n*, for β-CDEDTA (circles) and Hpβ-CDEDTA nanosponges (triangles and stars).

Journal of RAMAN SPECTROSCOPY

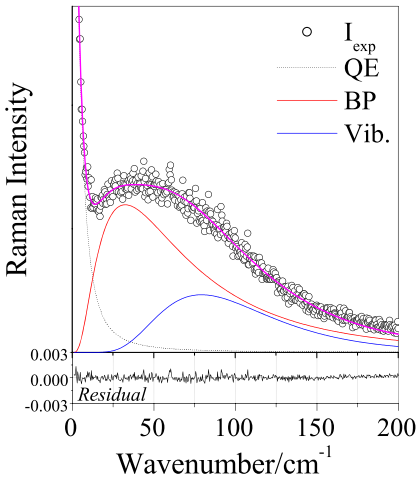

Figure 3. Low-wavenumber Raman spectrum of β-CDEDTA18 (empty circles) shown together with the total fitting curve (magenta line) and the different components resulting from the fitting procedure. From left to right: Lorentz function (dashed line) for the quasi-elastic (QE) contribution and two log-normal functional forms for the boson peak (BP) (red line) and higher-wavenumber vibrational modes (blue line). This figure is available in colour online at wileyonlinelibrary.com/journal/jrs.

In Fig. 3, the three different spectral components of the total experimental Raman profile $I(\omega)$ are evidenced by the fitting procedure[22]: a Lorentzian function, centered at zero wavenumber, with width ω_0 and amplitude A was used to reproduce the QE contribution and a log-normal distribution function with width W and amplitude B was employed to describe the shape and position of the maximum of BP, ω_{BP}. Finally, the contribution arising from higher-wavenumber vibrational modes, also present in the spectra, has been fitted by using another log-normal distribution function with width D, amplitude C, and peak wavenumber ω_{Vib} that well reproduces the asymmetric spectral shape of the band (see Eqn (1)).

$$I(\omega) = \frac{A\omega_0}{\omega_0^2 + \omega^2} + B \exp\left\{ -\frac{\left[\ln\left(\frac{\omega}{\omega_{BP}}\right)\right]2}{2W^2} \right\} + C \exp\left\{ -\frac{\left[\ln\left(\frac{\omega}{\omega_{Vib}}\right)\right]^2}{2D^2} \right\} \quad (1)$$

It is noteworthy that the choice of the log-normal function, although arbitrary, is quite standard to obtain in more quantitative way the position of the maximum of BP.[22,31,32,34,35]

In Fig. 4, the low-wavenumber Raman spectra of different samples of β-CDEDTA nanosponges are shown after the subtraction of QE contribution, which has been carefully carried out following the same method discussed in Ref. [22]. The spectra point out significant variations of the vibrational features of the experimental data. In particular, a clear evolution of the wavenumber of maximum BP as a function of molar ratio n is observed, suggesting a clear dependence of the stiffness of the polymeric network of nanosponges from the EDTA/CD molar ratio. The best-fit values of the wavenumber positions of the BP, ω_{BP}, estimated by using the data fitting procedure described earlier, are plotted as a function of n in the inset of Fig. 4 for the samples of EDTA-nanosponges examined.

It should be pointed out that the analysis here proposed allows us to better quantify the shifts observed for ω_{BP}, although the overall trend of the BP component is the same as that observed

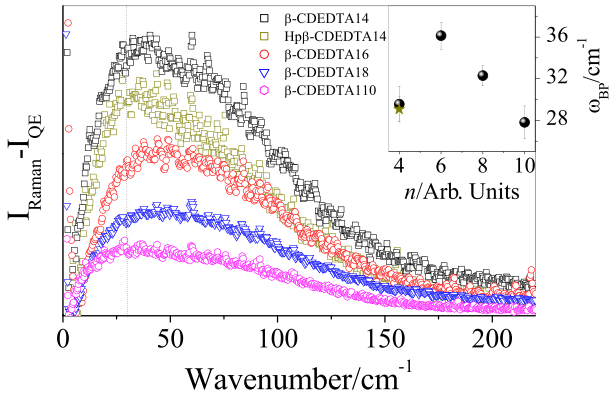

Figure 4. Raman intensity (after subtraction of I_{QE} contribution) for different samples of β-CDEDTA nanosponges, in the low-wavenumber region 0–200 cm^{-1}. The dotted vertical line indicates the wavenumber position of boson peak (BP) for the sample β-CDEDTA14. Inset: wavenumber position estimated for ω_{BP} as a function of the molar ratio n for β-CDEDTA (black circles) and Hpβ-CDEDTA nanosponges (dark yellow star). This figure is available in colour online at wileyonlinelibrary.com/journal/jrs.

in the spectral profiles of Fig. 4, thus confirming that the described fitting procedure does not affect the final results.

The wavenumber position of BP shows a maximum at molar ratio $n = 6$, whereas for higher values of n ω_{BP} tend to move to lower values, in agreement with the behavior already observed for C=O stretching band intensity. This trend suggests that, for $n < 6$, the increasing of the cross-linking degree of nanosponges is followed by a corresponding hardness of the polymeric network. Otherwise, beyond a sixfold excess of EDTA with respect to β-CD, the cross-linker probably provides branching of CD units, which prevents further cross-linking of the polymer and results in a general decreasing of the stiffness of the material. The data reported in the inset of Fig. 4 show also that the position of ω_{BP} for β-CDEDTA14 and Hpβ-CDEDTA14 does not change significantly, giving an indication that the cross-linking density and stiffness of the final polymer is mainly influenced by the amount of cross-linker rather than the type of CD macrocycle.

In Fig. 5, the position ω_{BP} estimated for nanosponges obtained by polymerization of β-CD with the three different cross-linking agents PMA, CDI, and EDTA are compared, as a function of n. The plots indicate a similar dependence on n of the stiffness of polymeric network for PMA-based and EDTA-based nanosponges, with a maximum of the rigidity observed for a sixfold excess of cross-linker with respect to the monomer β-CD. On

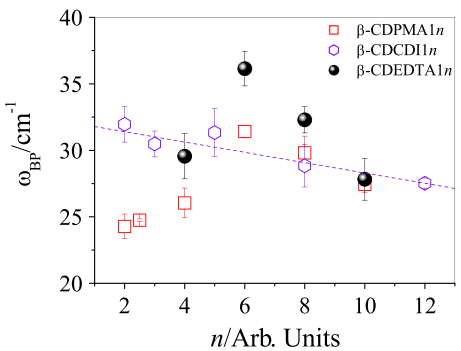

Figure 5. Evolution of ω_{BP} as a function of the molar ratio n for different types of nanosponges: β-CDPMA1n (empty squares), β-CDCDI1n (empty hexagons), and β-CDEDTA1n (closed squares).

the contrary, the saturation effect mentioned earlier is reached for a lower cross-linker/CD ratio ($n = 2$) in the carbonate-based nanosponges β-CDCDI1*n*, which show a systematic decrease of the wavenumber position of the BP with increasing the amount of CDI with respect to βCD.

Conclusion

The vibrational dynamics of polymeric networks obtained by polymerization of CD with the cross-linking agent EDTA is here investigated by the combined use of Raman and IR spectroscopies. The simultaneous analysis of different wavenumber regimes allowed to explore and compare between them the cross-linking degree and the elastic properties of this new class of polymers.

The detailed inspection of the spectral properties of the bands falling between 1600 and 1800 cm^{-1} in both Raman and IR spectra gave a relative estimation of the number of the C=O functional groups present in the polymeric network, in turn directly proportional to the degree of reticulation of the system. Finally, the observed changes in the wavenumber position of the so-called BP, a prominent feature found in the low-wavenumber Raman spectra of amorphous materials, provided important indications on the elastic properties of the polymeric matrix over a mesoscopic length scale.

The overall results provide an unprecedented characterization of the structural and dynamical properties of EDTA-nanosponges, confirming that the reticulation and the elastic properties of these polymers can be successfully modulated by acting on the relative amount of the cross-linker during the synthesis of the materials.

Acknowledgement

The author B. Rossi acknowledges the financial support of the Regione Veneto, being the beneficiary of a scholarship within the Programma Operativo Regionale FSE 2007-2013.

References

[1] F. Van de Manakker, T. Vermonden, C. F. Van Nostrum, W. E. Hennink, *Biomacromolecules* **2009**, *10*, 3157.
[2] Y. J. R. Tabata, *Soc. Interface* **2009**, *6*, S311.
[3] K. Sakurada, F. M. McDonald, F. Shimada, *Angew. Chem. Int. Ed.* **2008**, *47*, 5718.
[4] A. Atala, R. P. Lanza, J. A. Thomson, R. M. Nerem, Principles of Regenerative Medicine, Academic Press, Burlington (MA), **2008**.
[5] S. Li, W. C. Purdy, *Chem. Rev.* **1992**, *92*, 1457.
[6] J. Szejtli, *Chem. Rev.* **1998**, *98*, 1743.
[7] M. L. Bender, M. Komiyama (Eds.), Cyclodextrin Chemistry, Springer-Varlag, New York, **1978**.
[8] J. Szejtli (Ed.), Cyclodextrin Technology, Kluwer Academic Publishers, Boston, **1988**.
[9] D. Duchene (Ed.), New Trends in Cyclodextrins and Derivatives, Editions de Santè, Paris, **1991**.
[10] F. Trotta, W. Tumiatti, Patent WO 03/085002, **2003**.
[11] F. Trotta, W. Tumiatti, R. Cavalli, O. Zerbinati, C. M. Roggero, R. Vallero, Patent number WO 06/002814, **2006**.
[12] F. Trotta, R. Cavalli, *Compos. Interface.* **2009**, *16*, 39.
[13] R. Cavalli, F. Trotta, W. Tumiatti, *J. Incl. Phenom. Macro.* **2006**, *56*, 209.
[14] B. B. Mamba, R. W. Krause, T. J. Malefetse, G. Gericke, S. P. Sithole, *Water SA* **2008**, *34*, 657.
[15] M. Arkas, R. Allabashi, D. Tsiourvas, E. M. Mattausch, R. Perfler, *Environ. Sci. Technol.* **2006**, *40*, 2771.
[16] F. Trotta, W. Tumiatti, R. Cavalli, C. M. Roggero, B. Mognetti, G. Berta Nicolao, Patent WO 09/003656, **2009**.
[17] A. Vyas, S. Shailendra, S. Swarnlata, *J. Incl. Phenom. Macro.* **2008**, *62*, 23.
[18] S. Swaminathan, P. R. Vavia, F. Trotta, S. Torne, *J. Incl. Phenom. Macro.* **2007**, *57*, 89.
[19] B. Boscolo, F. Trotta, E. Ghibaudi, *J. Mol. Catal. B: Enzym.* **2010**, *62*, 155.
[20] S. Swaminathan, L. Pastero, L. Serpe, F. Trotta, P. Vavia, D. Aquilano, M. Trotta, G. Zara, R. Cavalli, *Eur. J. Pharm. Biopharm.* **2010**, *74*, 193.
[21] A. Mele, F. Castiglione, L. Malpezzi, F. Ganazzoli, G. Raffaini, F. Trotta, B. Rossi, A. Fontana, G. Giunchi, *J. Incl. Phenom. Macro.* **2011**, *69*, 403.
[22] B. Rossi, S. Caponi, F. Castiglione, S. Corezzi, A. Fontana, M. Giarola, G. Mariotto, A. Mele, C. Petrillo, F. Trotta, G. Viliani, *J. Phys. Chem. B* **2012**, *116*(17), 5323.
[23] F. Castiglione, V. Crupi, D. Majolino, A. Mele, B. Rossi, F. Trotta, V. Venuti, *J. Phys. Chem. B* **2012**, *116*(27), 7952.
[24] F. Castiglione, V. Crupi, D. Majolino, A. Mele, W. Panzeri, B. Rossi, F. Trotta, V. Venuti, *J. Incl. Phenom. Macro.* **2012**, DOI: 10.1007/s10847-012-0106-z.
[25] F. Castiglione, V. Crupi, D. Majolino, A. Mele, B. Rossi, F. Trotta, V. Venuti, *J. Phys. Chem. B* **2012**, *116*(43), 13133.
[26] S. N. Taraskin, Y. L. Loh, G. Natarajan, S. R. Elliott, *Phys. Rev. Lett.* **2001**, *86*, 1255.
[27] P. Benassi, A. Fontana, W. Frizzera, M. Montagna, V. Mazzacurati, G. Signorelli, *Phil. Mag. B* **1995**, *71*, 761.
[28] G. Baldi, A. Fontana, G. Monaco, L. Orsingher, S. Rols, F. Rossi, B. Ruta, *Phys. Rev. Lett.* **2009**, *102*, 195502.
[29] O. Pilla, L. Angelani, A. Fontana, J. R. Gonçalves, G. Ruocco, *J. Phys. Condens. Matter* **2003**, *15*, S995.
[30] A. Monaco, A. Chumakov, G. Monaco, W. A. Crichton, A. Meyer, L. Comez, D. Fioretto, J. Korecki, R. Ruffer, *Phys. Rev. Lett.* **2006**, *97*, 135501.
[31] K. Niss, B. Begen, B. Frick, J. Ollivier, A. Beraud, A. Sokolov, V. N. Novikov, C. Alba-Simionesco, *Phys. Rev. Lett.* **2007**, *99*, 055502.
[32] L. Hong, B. Begen, A. Kisliuk, C. Alba-Simionesco, V. N. Novikov, A. P. Sokolov, *Phys. Rev. B* **2008**, *78*, 134201.
[33] S. Caponi, S. Corezzi, D. Fioretto, A. Fontana, G. Monaco, F. Rossi, *Phys. Rev. Lett.* **2009**, *102*, 027402.
[34] L. Hong, P. D. Gujrati, V. N. Novikov, A. P. Sokolov, *J. Chem. Phys.* **2009**, *131*, 194511.
[35] M. Zanatta, G. Baldi, S. Caponi, A. Fontana, E. Gilioli, M. Krish, C. Masciovecchio, G. Monaco, L. Orsingher, F. Rossi, G. Ruocco, R. Verbeni, *Phys. Rev. B* **2010**, *81*, 212201.
[36] V. Crupi, G. Guella, D. Majolino, I. Mancini, A. Paciaroni, B. Rossi, V. Venuti, P. Verrocchio, G. Viliani, *Phil. Mag.* **2011**, *91*, 1776.